

The Solar Particle Access Model (SPAM): A new tool for monitoring solar energetic particle impacts to satellite operations

J.C. Green

Space Hazards Applications, LLC

T.P. O'Brien¹, R. Quinn², S. Huston³, P. Whelan³, N. Reker²

(1) The Aerospace Corporation, (2) Atmospheric and Environmental Research, (3) Space Hazards Applications, LLC

Abstract

The number of satellites in Low Earth Orbit (LEO) or Medium Earth Orbit (MEO) is growing rapidly to support critical services such as internet and detailed imaging. At these altitudes, satellites may be protected from some space particle radiation but are still vulnerable to impacts from Solar Energetic Particles (SEPs). The application described in this work is intended to help satellite operators monitor and mitigate possible effects from these particles on satellites. SEPs are a highly sporadic component of space radiation comprised of extremely energetic protons and heavy ions. They are produced in shock fronts that steepen ahead of Coronal Mass Ejections (CMEs) intermittently released from the Sun. Once they reach Earth, these high energy ions can easily pass through outer satellite shielding and damage electronic components, resulting in temporary malfunctions, degraded performance, or a complete system or mission loss. Most satellites are designed to tolerate these relatively infrequent events, but unexpected issues still occur especially during intense SEPs that may exceed design thresholds. Many of the new satellite mega-constellations may have unknown vulnerabilities because they were launched after the most recent large SEP events. The impacts to satellite operations from a large SEP may be further exacerbated because the events are likely to coincide with other intense space weather that changes atmospheric drag and creates tracking challenges. When an SEP occurs, it is necessary to define the regions of near-Earth space that will be most impacted. Some of the ions are deflected by Earth's magnetic field creating partially shielded regions. Identifying which satellites are at risk for SEP related anomalies in LEO/MEO orbit is currently challenging because there are no easily available real time models and tools for defining where these energetic protons have access. To provide such monitoring information, we are developing the Solar Particle Access Model (SPAM). The model describes solar particle access at Earth by mapping real time measurements of high energy ions from low altitude satellites throughout the magnetosphere. It will be made available through an online application to easily deliver actionable information to users.

1. Introduction

Satellites in space are continuously subjected to intense particle radiation that can damage components and cause anomalous behavior or a sudden and complete loss of function. The radiation intensity and its effect on satellite systems will vary depending on the exact satellite location, its design, and the level of space weather activity in the massive and connected magneto-hydrodynamic system that extends from the sun to the outer solar system. The potential large-scale impacts from space weather on the global satellite fleet are now heightened as the number of satellites, particularly in low and medium Earth orbit (LEO and MEO), steadily increases. At these altitudes, precise

tracking and coordination of satellite orbits is necessary to avoid collisions that could produce cascading and untenable amounts of debris. An intense space weather event may complicate this intricate coordination effort. During such an event, satellite trajectories will be altered and difficult to predict due to space weather induced changes in the atmospheric density and drag. At the same time, some communication and commanding abilities needed to change the course of a satellite to avoid a collision may be lost due to effects from enhanced space radiation. This work describes the development of a new space radiation model and an online application for accessing that model output in order to better monitor, anticipate, and respond to potential impacts to satellites from space weather events.

The space radiation environment is a constant threat to routine satellite operations that must be monitored and mitigated for successful missions. Generally, that threat is relatively well characterized by climatological models (e.g. the IRENE model [1]) that can describe the expected distribution of particle radiation intensities and extremes over a satellite's planned lifetime. Some satellite engineers will use these climatological models to estimate expected radiation levels prior to launch and provide sensitive electronics with sufficient shielding to avoid unwanted impacts. However, on-orbit satellite anomalies may still occur due to unexpected design features or environments that exceed chosen design thresholds. Our goal is to provide tools to understand and anticipate when and where these anomalies are most likely to occur once satellites are on orbit. To achieve this goal requires an understanding of the space radiation environment, the physics controlling its intensity, and the expected impacts to specific satellite systems. Experience and experimental testing have shown that there are 4 different types of effects that are each caused by different components of the space particle radiation environment (see Table 1.0). Interestingly, intensifications of the different particle components and their related effects are not simultaneous in time or location. For example, the low energy particle flux (related to surface charging) is most likely to increase at GEO during magnetic substorms which may occur sporadically on average every 3 hours. (A substorm is a sudden reconfiguration of the Earth's magnetic field in the extended nightside region which can accelerate and transport particles Earthward). Whereas, single event effects (SEE's) are more likely to occur when the sun releases a very large magnetic structure known as a coronal mass ejection (CME). The CME will create a shock front as it plows outward from the sun through the heliosphere. Ions in the ambient space are accelerated as they move through the shock and will travel ahead of the CME towards Earth. As a result, SEEs from such an event may be observed days prior to the onset of any other enhanced geomagnetic activity once the CME reaches Earth. Thus, in order to specify the threat from each of these impacts requires separate models that capture the physics of each radiation component. Previously, we have focused our attention on tools and science for specifying the high energy electron environment and internal charging effects [2][3]. To expand that work, our specific focus here is on developing a model that defines the location and likelihood of SEEs caused by these CME induced solar energetic particle events (SEPs).

Table 1.0 Space Weather Related Anomalies

Radiation	Effect	Description	Space Weather Cause
Low energy protons/ electrons (<50 keV)	Surface Charging	Charged particles collect on satellite surfaces producing high voltages, damaging arcs, and electromagnetic interference. Common problem areas- thermal blankets, solar arrays.	Ring current particle fluxes intensify during storms and substorms
High energy electrons (>100 keV)	Internal Charging	Energetic electrons accumulate in interior dielectrics (circuit boards/cable insulators) and on ungrounded metal (spot shields/ connector contacts) leading to electrical breakdown near sensitive electronics.	Electron radiation belts intensify during fast solar wind, Corotating Interaction Regions, Coronal Mass Ejections
Energetic ion/protons (MeV)	Single Event Effect (SEE)	Energetic charged ion passage through microelectronic device node causes instantaneous device failure, latent damage, or uncommanded mode / state changes requiring ground intervention.	Trapped proton belts (L<~3.5) and Solar Energetic Particle events (SEPs)
Energetic ions electrons (MeV)	Total Ionizing Dose (TID)	Energy loss (deposited dose) from proton/ electron passage through microelectronic device active region builds over mission (or step-wise during large events) causing device degradation and reduced performance at circuit/system level.	Electron radiation belts, trapped proton belts, SEPs

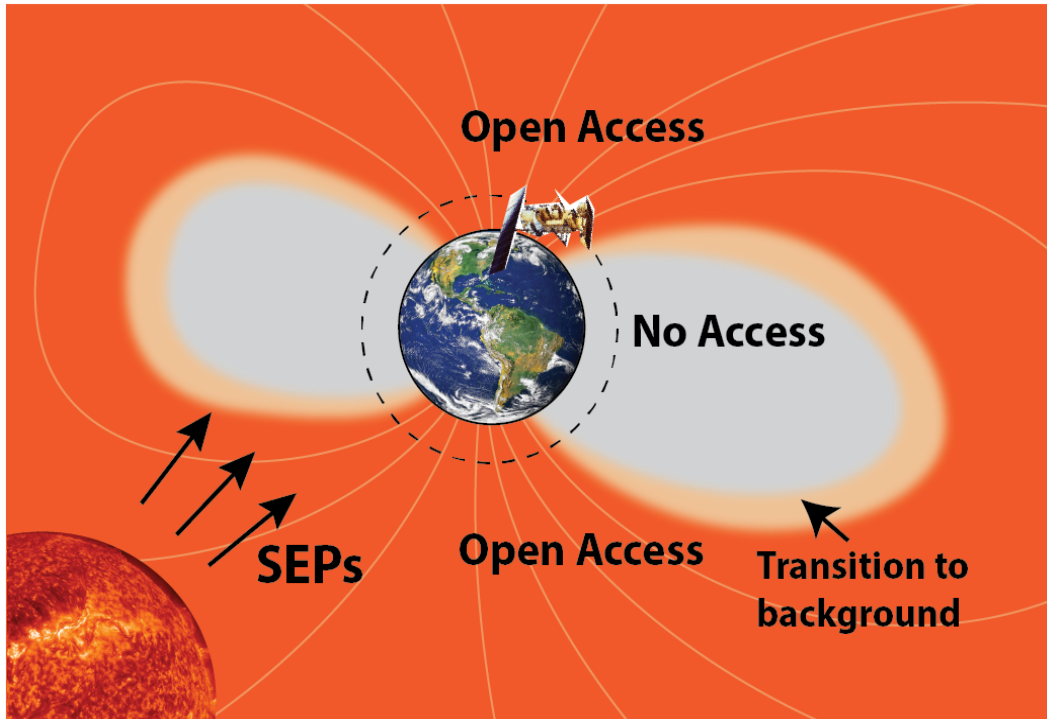


Fig 1. Schematic showing solar proton access near Earth

In recent years, the number and location of satellites orbiting Earth has changed dramatically which impacts the development and focus of any radiation model. While the total number of satellites continues to increase in all orbits, those in LEO now greatly outnumber the population in other regions (3327 LEO satellites, 519 GEO satellites, 137 MEO satellites [4]). The concentration of satellites in LEO means that any radiation and effects models must accurately specify this region. This point is particularly important for models of particle radiation from SEP events. As mentioned previously, these high energy ions stream towards and engulf the Earth as CMEs are launched from the sun. However, once the ions reach Earth, their impact is not uniform across all locations and orbits. Over the high latitude polar cap regions, where magnetic field lines connect from the Earth directly to the solar wind, the ions have unimpeded access all the way down to the atmosphere. At lower latitudes, the magnetic field lines become more curved, and the ions are deflected. This means that some regions close to Earth and at low latitudes will be safe from these ion impacts as depicted in Fig 1. Additionally, these access regions change as the magnetic field is continuously pushed and distorted by structures in the solar wind that emanates from the sun. Thus, to understand the threat to a satellite at a given time requires a clear definition of these fluctuating access regions relative to the satellite location. The point of our new model, the Solar Particle Access Model (SPAM), is to do just that.

Several models currently exist that, like SPAM, attempt to define the regions where SEPs have access. However, these existing models were not all developed specifically for satellite anomaly attribution and so have limitations for this particular task. For example, some are not global and/or have limited accuracy. None are readily available and accessible in real time for satellite operators interested in understanding observed impacts to specific assets on orbit. Current models fall into 3 categories which all have different strengths and weaknesses: physics-based, simplified physics, and statistical. The physics-based models [5] define ion access by tracing trajectories of ions of different energies and species outward from a sampling of locations and directions in a global magnetic field model. If the tracing shows that a particle can make it out from a particular location and direction then likewise ions streaming from the sun will have access. This method for determining access is potentially very accurate but is dependent on the model magnetic field accuracy which is often difficult to quantify. The method is also computationally

expensive if used with a sophisticated time varying magnetic field model because the particle trajectories must be continuously re-calculated. Because of the computational challenge, this type of technique is generally not used to define global access such as is needed for satellite anomaly monitoring. The technique can be simplified by pre-calculating particle trajectories and access regions in a set number of magnetic field configurations [6,7]. This simplified physics technique makes the tracing problem feasible but now less accurate. Finally, statistical methods use large numbers of observed SEP events to determine how access regions vary with geomagnetic activity indicators such as the Dst or Kp index. For example, one statistical model [8] used measurements from the SAMPEX satellite to define the latitude at which the ion flux over the polar cap is expected to drop by 50% for different levels of the geomagnetic activity. (This boundary location is sometimes referred to as the cutoff location or cutoff latitude). While the cutoff location is easily defined at the altitude of the SAMPEX satellite (~ 670 km), it is unclear how this boundary maps to higher altitudes. Additionally, during intense events, satellites may have anomalies when the flux drops to much less than 50% of the maximum level. Finally, comparison of these different types of model predictions to one SEP event that was well observed with detailed measurements from the Van Allen probes calls into question the accuracy of these methods [9]. The analysis in that study showed that the techniques capture the average location of the access regions but they do not capture the idiosyncratic variability of individual storms.

Our goal with the SPAM model is to address these issues and create a global real time specification of ion access and SEE rates specifically targeted for use by satellite operators for anomaly monitoring, attribution, and analysis. To avoid any ambiguity regarding the location of access regions, the SPAM model relies on real time observations of the access from a suite of low altitude satellites. This technique captures the variability of the access regions even during extreme or infrequent events that are often averaged out using other methods. To make the model global, we compare access regions observed by satellites at different magnetic local times (MLT) and altitudes. Those comparisons are used to define functions for mapping the low altitude observations throughout the magnetosphere. Finally, the model output will be transformed into actual satellite effects (SEE rates) for user specific satellite orbits, components, and designs and will be incorporated into the framework of the existing Satellite Charging Assessment Tool (SatCAT) for easy real time access.

2. DATA

In order to create SPAM, we rely on proton measurements from both low and high altitude satellites. To sample the low altitude region, we use data from the Polar Orbiting Environmental Satellites (POES) operated by the National Oceanic and Atmospheric Administration (NOAA) and the Meteorological Operational Satellites (MetOp) operated by the European Organization for the Exploitation of Meteorological Satellites (EUMETSAT). Both these satellite suites carry Space Environment Monitors (SEM) that include the Medium Energy Proton and Electron Detector (MEPED). To sample the highest energy protons, the MEPED has a set of omnidirectional dome detectors that measure the flux of protons in 4 energy bands (p6 >16 MeV, p7 >35 MeV, p8 >70 MeV, p9 >140 MeV omnichannels [10]). We use data from the SEM-2 version of the instruments which provides data from 1998 to the present (<https://www.ngdc.noaa.gov/stp/satellite/poes/dataaccess.html>).

To sample the high altitude region, we use data from the Highly Elliptical Orbit (HEO) F3 satellite. The satellite measures protons in 4 energy bands (p4 >5 MeV, p5 >8.5 MeV, p6 >16 MeV, and p7 >27 MeV) and is in a ~1.15 x 7.2 Re orbit inclined at ~63° with a ~12-h period. The data are currently available at the Virtual Radiation Belt Observatory (<https://science.nasa.gov/heliophysics/heliophysics-data-centers/virtual-radiation-belt-observatory-virbo>)

3. METHOD

Our goal is to specify the global (all latitudes, longitudes, and altitudes) ion flux near Earth throughout an SEP event using only measurements from the POES/MetOp satellites that each sample only a single track through the

environment at a fixed altitude (~850km). (Typically, the data are telemetered to the ground once per orbit. With 6 satellites currently in operation, the data downloads will allow the model to update approximately once every 20 minutes.) Fig. 2 shows proton flux sampled from one POES satellite (NOAA-15) and serves as an example of the input data to the model. Understanding this input is necessary to appreciate how this limited observation is mapped out to a global environment as described in the next sections. The data in Fig. 2 are plotted as proton flux versus L shell. (L shell is a magnetic coordinate that organizes particle data in a magnetic field better than more standard geophysical coordinates such as latitude and longitude. It is approximately the radial distance from Earth at which a particle that is trapped in the magnetic field will cross the equator.) The figure demonstrates how the proton flux is typically organized during an SEP event. At large L shells (high latitudes) the proton flux is high because the structure of the magnetic field over the polar caps allows the protons streaming from the sun direct access down to the atmosphere. The flux decreases to low background levels as the satellite moves equatorward to smaller L shells (lower latitudes) because the ions are now completely deflected by the magnetic field. This pattern will then repeat in reverse as the satellite moves from the equator back to higher latitudes and L shells. To map a single pass of data like that shown in Fig 2. to all locations requires two steps. First, that flux profile must be mapped around the Earth to all magnetic local times (MLTs) still at the same POES altitude. Next the flux must be mapped from the low altitude of POES out to higher altitudes as described in more detail in the next sections.

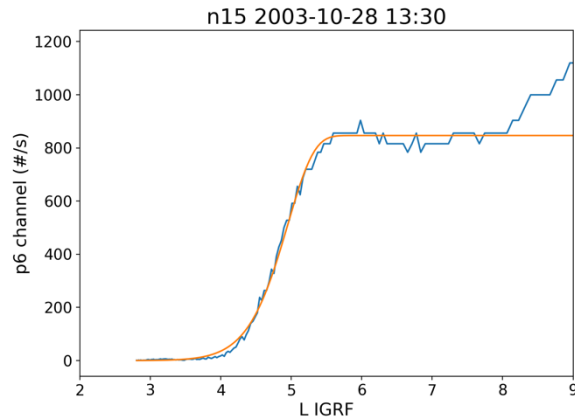


Fig. 2. Example showing proton flux (p6 channel) as a function of L-shell measured by the NOAA-15 POES satellite along with a Weibull fit (orange) during a 2003 SEP event

3.1 MLT Dependence

For the first mapping step we compare simultaneous low altitude measurements at different MLTs to derive a functional relationship between the locations. This step can be done using measurements from all the POES/MetOp satellites that orbit in different planes. To simplify the comparison, we first fit each pass of data to a Weibull function as given below:

$$J(L) = J_0 \left(1 - \exp \left[- \left(\frac{L}{L_0} \right)^\gamma \right] \right)$$

Here J is the flux and L is the L shell. The 3 parameters to be fit are L_0 , J_0 and γ . The L_0 parameter describes the location where the flux drops to 63% of the maximum value, γ describes the steepness of the decrease, and J_0 describes the maximum flux at high latitudes. The orange trace in Fig. 2 shows an example of one such Weibull fit to the data.

POES/MetOp p6 channel 2005-09-08

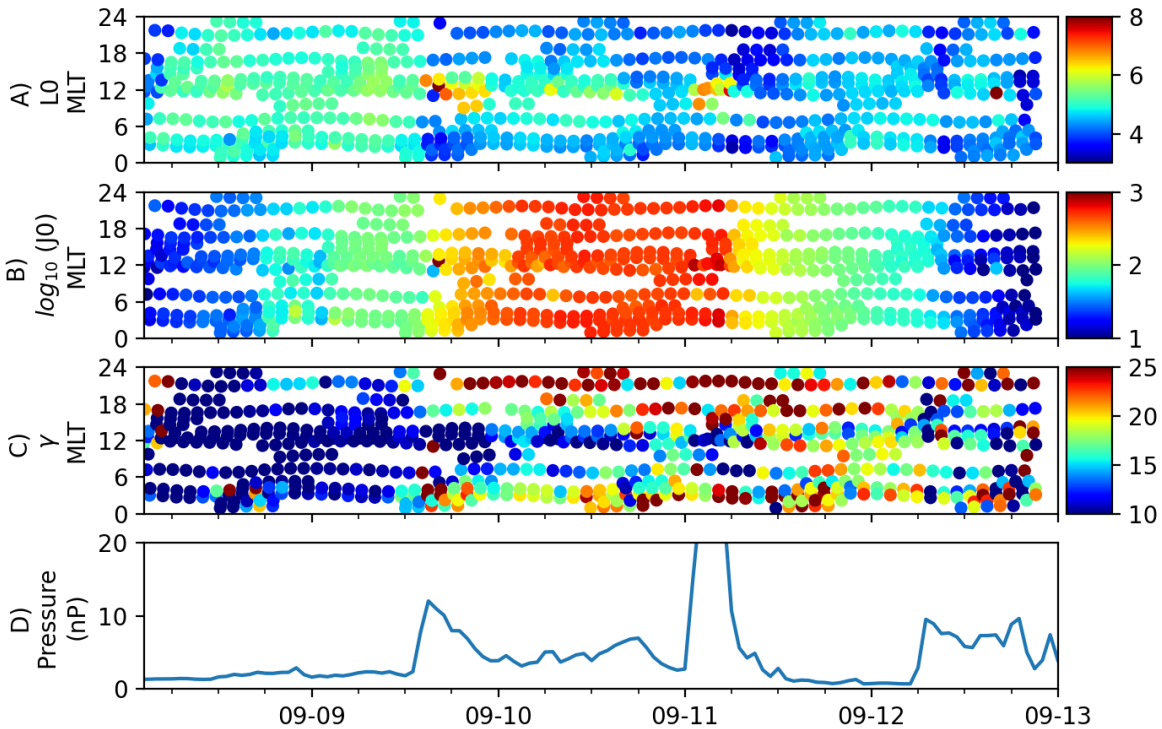


Fig.3. Parameter fit values during one SEP event (2005-09-08) as a function of time and MLT from 6 POES/MetOp satellites. Panels A, B, C show the fit values L_0 , J_0 , and γ respectively and panel D shows the solar wind dynamic pressure (nP).

Now comparing passes at different MLTs is a matter of comparing the fitted parameters. To demonstrate, Fig. 3 shows how the fit parameters vary as a function of MLT and time during one SEP event in 2005. For this event, data from 6 POES/MetOp satellites was available giving good MLT coverage. The plot shows a noticeable connection between the dynamic pressure of the solar wind pushing on the magnetosphere and the proton access described by the L_0 parameter (dynamic pressure = $\rho_{\text{solar_wind}} v^2_{\text{solar_wind}}$ where $\rho_{\text{solar_wind}}$ is the solar wind density and v is the solar wind velocity). Other geomagnetic indices did not show as strong of a correlation. When the dynamic pressure is low ($< \sim 3$ nP), the proton flux reaches into $L_0 \sim 4$ uniformly at all MLT. When the dynamic pressure increases, the dayside magnetosphere is compressed and the magnetic field strength increases which more easily deflects the incoming ions. As a result, the access is no longer uniform around the Earth. The access moves outward to $L_0 > 6$ on the dayside (MLT $\sim 12-14$) but inward everywhere else. The other two fit parameters (J_0 and γ) show no obvious correlation with MLT or geomagnetic activity.

In order to better quantify the variation in ion access and its dependence on the dynamic pressure, we combine measurements from all SEP events from 1998 to 2021 as shown in Fig. 4. Here we bin the L_0 values for all events as a function of MLT and dynamic pressure. After binning, we divide the values by the maximum L_0 at each dynamic pressure value and then use a Gaussian smooth to reduce noise. The binned data captured in the plot now gives us a means for mapping from one MLT to another. For example, if one satellite observes a flux profile with $L_0 = 7$ at 12 MLT when the pressure is > 8 nP, then the L_0 value at 21 MLT would be .75 times that (or $L_0 = .75 \times 7 = 5.25$).

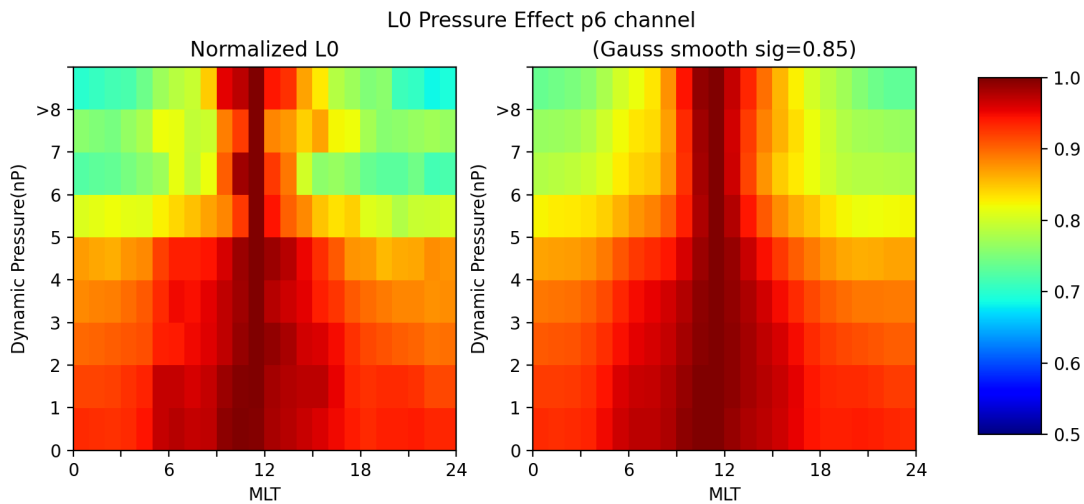


Fig. 4. Depiction of the change in the ion access as a function of the solar wind dynamic pressure. The left panel shows L_0 fit parameters binned as a function of pressure (nP) and MLT and normalized by the maximum L_0 in each dynamic pressure bin. The right panel shows the same data now smoothed with a Gaussian smooth.

To assess how well the mapping in MLT works we compare the L_0 fit parameters measured at NOAA-15 to those from other POES/MetOp satellites when the measurements are within 5 minutes. The results of the comparison are given in Fig. 5. The left panel shows a direct comparison between the L_0 values measured at NOAA-15 to the other satellites with no mapping and the right panel shows the same after the mapping has been applied. Using the mapping procedure, the correlation between the two increases from $r^2=.53$ to $r^2=.73$ and the RMS error reduces from .42 to .30 demonstrating a significant improvement.

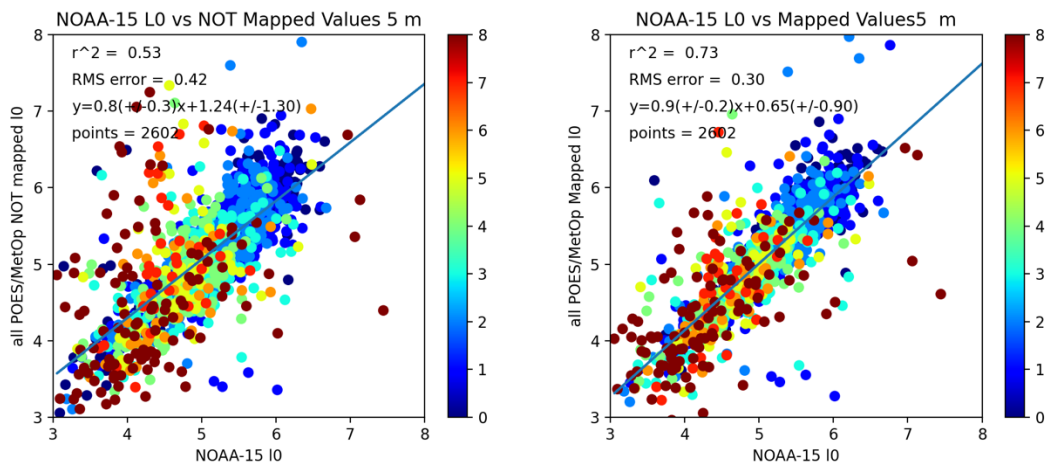


Fig. 5. Comparison of L_0 fit parameters measured by NOAA-15 to those measured by other POES/MetOp satellites. The left panel shows a comparison between the L_0 parameters measured at NOAA-15 (x-axis) and the L_0 parameters measured at the other satellites (y-axis) with NO mapping. The right panel shows the same but now the L_0 parameters measured at the other satellites are mapped to the MLT of the NOAA-15 satellite. Each point is color coded by the dynamic pressure at the time of the observation.

3.2 Altitude Dependence

The next step is to compare data at different altitudes to understand how the flux can be mapped outward from the location of the POES/MetOp satellites. To do so, we compare simultaneous measurements (within 10 minutes) from POES/MetOp and the HEO F3 satellite which is in a highly elliptical orbit. We also restrict the analysis to channels on each satellite that measure protons with similar energies. We expect access regions to vary with energy because higher energy protons have larger gyroradii and will not be as easily deflected by Earth's magnetic field. Again, to simplify the comparison, we fit the individual passes of both datasets to Weibull functions (as in Fig. 2) and compare the fit parameters. Most often the POES/MetOp and HEO satellites are not at the same MLT when making close measurements. To account for this difference, we first map the POES/MetOp L_0 fit parameters to the same MLT as HEO using the method described above. The results of this comparison between the L_0 fit parameters for the POES/MetOp >35 MeV protons and the HEO >27 MEV protons are shown in Fig 6. The regression of the L_0 values between the two satellites gives $y=1.1(+/-0.1)x+0.32(+/-0.63)$ and demonstrates a nearly one to one correspondence between the profiles at the two completely different altitudes. This relationship indicates that we can map the profiles measured at POES/MetOp along field lines or L shells to other altitudes.

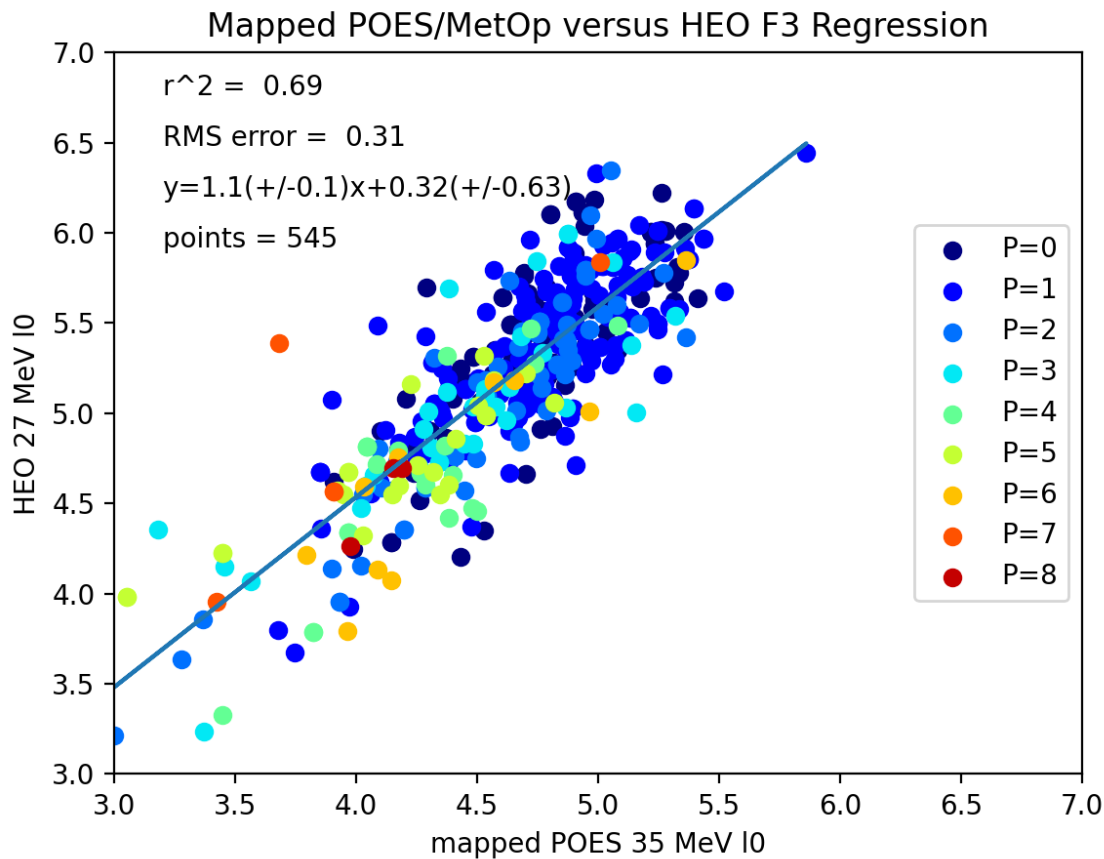


Fig 6. Comparison of the L_0 fit parameters obtained from the POES/MetOp satellites 35 MeV proton channel (x-axis) and the HEO F3 27 MeV proton channel satellite (y-axis). Each point is color coded by the solar wind dynamic pressure (nP) at the time of the measurement as shown in the legend. The POES/MetOp L_0 values are mapped to the MLT of the HEO F3 satellite using the procedure described in section 3.1.

3.3 Mapping Procedure and Application

The results described above now give us a means for mapping the low altitude POES/MetOp observations during an SEP event to any target satellite location and time. The method for mapping is as follows:

- 1) Retrieve any available POES/MetOp 35 MeV proton flux for the time period of interest
- 2) Fit each pass to a Weibull function
- 3) Map the POES/MetOp L_0 values to the MLT of the target satellite
- 4) Find the flux $J(L)$ at the L-shell of the target satellite using the most recent mapped POES/MetOp fit parameters

This algorithm has now been implemented into the online SatCAT system for evaluation and will be available to outside users for routine operations within the next year. The application allows users to choose any satellite of interest from the NORAD satellite catalog. It generates a trajectory for that satellite and calculates the proton flux along the orbit in order to create a time history for evaluation during an SEP event. It will also collect new data and update in real time for continuous monitoring of any threat. The algorithm is currently being expanded to include other ion species and energies which may also cause SEEs. In addition, the algorithm will include the option to translate the ion flux levels into the specific impact (SEE rate) for different component designs which is more meaningful for satellite operations.

4. SUMMARY

Impacts from solar energetic particle events can cause unexpected behavior and damage to satellites on orbit. These types of events have the potential to cause large scale disruptions to routine operations and leave satellites incommunicable at critical times when collision risks due to changes in atmospheric drag are also elevated. The SPAM model described here provides a global specification and describes how the solar particle impacts vary as a function of both time and location. The model captures the highly variable nature of the events and reduces uncertainty by relying on real time observations of proton fluxes at low altitudes as the primary driver. The output will be made available through an easy to access online application that can be tailored to give the expected threat to users specified satellites and component designs. The SPAM output will provide satellite operators and engineers with a tool to monitor, analyze, and manage the real time risk from these solar particle events.

1. REFERENCES

- [1] Ginet, G.P., T.P. O'Brien, S.L. Huston, W.R. Johnston, T.B. Guild, R. Friedel, C.D. Lindstrom, C.J. Roth, P. Whelan, R.A. Quinn, D. Madden, S. Morley and Yi-Jiun Su, AE9, AP9 and SPM: New Models for Specifying the Trapped Energetic Particle and Space Plasma Environment, *Space Science Reviews*, March 2013. [<http://dx.doi.org/10.1007/s11214-013-9964-y>]
- [2] Green, J. C., J. Likar, and Y. Shprits, Impact of space weather on the satellite industry, *Space Weather*, 15, 804–818, 2017, doi: [10.1002/2017SW001646](https://doi.org/10.1002/2017SW001646).
- [3] Green, J. C., R. Quin, P. O'Brien, J. Likar, Y. Shprits, S. Huston, A. Boyd, S. Claudepierre, P. Whelan, N. Reker, Developing a Comprehensive Application for Satellite Anomaly Analysis and Attribution, AMOS Conference, 2020.
- [4] Union of Concerned Scientists (UCS), <https://www.ucsusa.org/resources/satellite-database>, updated May 1, 2021

- [5] Kress, B. T., M. K. Hudson, R. S. Selesnick, C. J. Mertens, and M. Engel, Modeling geomagnetic cutoffs for space weather applications, *J. Geophys. Res. Space Physics*, 120, 5694–5702, 2015, doi:10.1002/2014JA020899.
- [6] Smart, D. F., and M. A. Shea, The space-developed dynamic vertical cutoff rigidity model and its applicability to aircraft radiation dose, *Adv. Space Res.*, 32(1), 103–108, 2003, doi:10.1016/S0273-1177(03)90376-0.
- [7] Smart, D. F., M. A. Shea, A. J. Tylka, and P. R. Boberg, A geomagnetic cutoff rigidity interpolation tool: Accuracy verification and application to space weather, *Adv. Space Res.*, 37(6), 1206–1217, 2006, doi:10.1016/j.asr.2006.02.011.
- [8] Leske, R. A., R.A. Mewaldt, E.C. Stone, T.T., von Rosenvinge, Observations of geomagnetic cutoff variations during solar energetic particle events and implications for the radiation environment at the Space Station, *Journal of Geophysical Research*, 106(A12), 30,011–30,022, 2001, <https://doi.org/10.1029/2000JA000212>.
- [9] O'Brien, T. P., J. E. Mazur, M. D. Looper, Solar energetic proton access to the magnetosphere during the 10–14 September 2017 particle event, *Space Weather*, 16, 2022–2037, 2018, <https://doi.org/10.1029/2018SW001960>.
- [10] Machol, J., POES/METOP SEM-2 OMNI Flux Algorithm Theory and Software Description, 2012, available at https://www.ngdc.noaa.gov/stp/satellite/poes/docs/NGDC/MEPED_OMNI_processing%20ATBD_V1.pdf.